Desalination and Water Treatment
www.deswater.com

36 (2011) 334–343
December

1944-3994/1944-3986
doi: 10.5004/dwt.2011.2521

Removal of Cr (VI) from aqueous solution using MCM-41

Lin Tian[a], Gang Xie[a]*, Rong-xing Li[a], Xiao-hua Yu[a], Yan-qing Hou[a]

[a]*Faculty of Metallurgical and Energy Engineering, Kunming University of Science and Technology, Kunming 650093, PR China*
Tel.: +868715186166; Fax: +86871518616; email: gangxie@sina.com

A B S T R A C T

Mesoporous molecular sieves (MCM-41) was successfully synthesized using hydrothermal synthesis and characterized by X-ray diffraction and nitrogen adsorption–desorption. Characterization results show that synthesized MCM-41 is a good adsorption material of good crystallinity, large surface area (1,040 m^2/g) and uniform diameter (centered at 2.8 nm). Removal of Cr (VI) from aqueous solution using MCM-41 was carried out by UV-Vis spectrophotometry. The different parameters affecting the adsorption efficiency were investigated and obtained their optimal values (pH 4, temperature 35°C, initial Cr (VI) concentration < 10 mg/L, adsorption time 2 h, adsorbent concentration of 10 mg/L). It is very useful and important to deal with Cr (VI) from aqueous solution. The adsorption isotherm was also investigated. It is found that the adsorption isotherm follows the Langmuir model better. What's more, b of 76.71 mg^{-1} and q of 904 mg/g were calculated from Langmuir linear fitting. The adsorption reaction is spontaneous and endothermic as $\Delta G^0 < 0$ and $\Delta H^0 > 0$. Finally, we studied the adsorption kinetics and find that the adsorption of Cr (VI) ions onto MCM-41 is more suitable for pseudo-second-order kinetics. q_e and k_2 were calculated. The detailed kinetic mechanism is that film diffusion is its mainly controlling step, but intra-particle diffusion is a considerable contribution to adsorption mechanism, which must be meaningful to accelerate adsorption rate.

Keywords: MCM-41; Chromium (VI); Adsorption isotherm; Adsorption thermodynamics; Adsorption kinetics

1. Introduction

With social and economic development, heavy metal contaminated water has been released directly into the environment, especially in China, which cause water and soil pollution [1,2]. One of the most important heavy metals is Cr (VI), because Cr (VI) leads to many diseases and seriously threatens human health [3]. Almost all the countries in the world have legislated on the standard of discharge of industrial Cr (VI) wastewater. For example, the US EPA permits Cr (VI) levels of 0.05 and 0.1 mg/L in drinking water and inland surface water, respectively. Therefore, wastewater containing chromium must be treated to be allowable limits before discharge into the environment. Currently, the main methods of removing heavy metal ions from water are activated carbon adsorption [4], ion exchange [5], ultrafiltration [6], reverse osmosis [7], electrodialysis [8], etc. These processes are expensive and have high reagent and energy requirements, suffer from incomplete metal removal, and generate a large quantity of toxic waste sludge, which necessitates careful disposal in further steps [9]. Therefore, the search for economical, easily available and highly efficient adsorbent is of interest. Molecular sieves including MCM-41 have received plenty of attentions for

*Corresponding author

use in the ion exchange process [10–12] during water treatment.

MCM-41 was initially studied and developed to be a new type of mesoporous material (Beck et al., 1992) by the American Mobile Company in 1992. Since then, MCM-41 has subsequently been optimized and used for the adsorption of several heavy metals [13–16]. For example, Mahitti and Fuangfa [17] used chemically modified MCM-41 to adsorb Hg (II) ions. Only few studies [18,19] on the adsorption of Cr (VI) from aqueous solution using MCM-41 have been undertaken. Lam's [18] and Ghiaci's [19] researches shown that MCM-41 was an efficient adsorbent for adsorbing Cr (VI) from aqueous solution. But neither of them systematically studied influencing factors, thermodynamics and kinetics of adsorption. Some scientists have used walnut hull [20], activated carbon [21] and other materials to adsorb Cr (VI), but these materials adsorption rates are low. MCM-41 might be a good material for the adsorption of Cr (VI) because of its uniform pores, narrow size distribution, high specific surface area and wall thickness, adjustable aperture, high chemical stability and thermodynamic stability [22]. In the paper, we used laboratory-made MCM-41 to adsorb chromium ions from aqueous solution. Influencing factors, thermodynamics and kinetics of adsorption were systematically studied. Finally, we determined the optimal condition, thermodynamics and kinetics of adsorbing Cr (VI) from aqueous solution, especially controlling step, which is very important for industrial use. It is also the goal of this work.

2. Experimental

2.1 Synthesis and characterization

Mesoporous MCM-41 was successfully prepared using different synthetic procedures and conditions [23]. For this study, the preparation of MCM-41 powder used hydrothermal synthesis with cetyltrimethylammonium bromide (CTAB, 99%), tetraethylorthosilicate (TEOS), ammonia (98%) and deionized water in a mass ratio of 1 CTAB: 4.5TEOS: $25H_2O$: $12NH_3{\cdot}H_2O$. After crystallization at room temperature (25°C) for 48 h, the MCM-41 powder was then filtered, washed, and dried before it was calcined in a furnace at 550°C for 5 h to remove the organic template. X-ray diffraction (XRD) patterns (Rigaku) was used to characterize MCM-41 at 35 kV, 20 mA and Cu-Kα radiation. Nitrogen adsorption–desorption isotherms were measured using a Micromeritics ASAP 2020M, and pore size distributions were calculated using the Barrett-Joyner-Halenda (BJH) method from the desorption branch. Specific total surface areas were calculated using the Brunauer-Emmet-Teller (BET) equation. The ultraviolet-visible (UV–Vis) spectrophotometer made in Beijing Rayleigh Analytical Instruments Inc was to analyze the residual Cr (VI) in the solution.

2.2. Adsorption experiments

The chromium ion concentrations range from 2.5 to 50 mg/L were obtained after dissolving potassium dichromate (AR) in deionized water. Then solution pH was adjusted by industrial sulfuric acid (H_2SO_4 98%, ammonia 98%) at certain Cr (VI) concentration and solution volume. Thirdly, the solution added some MCM-41 was stirred (150 rpm) at certain time and temperature. Fourthly, the MCM-41 powder was filtered and the residual Cr (VI) in the solution was analyzed using UV-Vis spectrophotometry [18–20]. Single factor experiments were then carried out when required. For example, to examine the effects of pH on chromium ion adsorption, pH is adjusted by industrial sulfuric acid (H_2SO_4 98%) and ammonia (98%) range from 1 to 8 at an adsorbent dosage of 10 mg/L, initial Cr (VI) concentration of 10 mg/L and 25°C for 3 h. After adsorption, the MCM-41 powder was filtered and the residual Cr (VI) in the solution was analyzed using UV–Vis spectrophotometry. The optimal pH for the removal of chromium (VI) was determined and the other experimental conditions were determined using a single factor experiment.

2.3. Adsorption efficiency and capacity

Some basic functions can be formulated as follows:

$$\text{Adsorption efficiency} = \frac{C_0 - C_t}{C_0} * 100\% \quad (1)$$

$$\text{Adsorption capacity } q_t : q_t = \frac{(C_0 - C_t)}{m} * V \quad (2)$$

where q_t is the adsorption capacity of per unit mass of chromium ion of adsorbent (mg/g) at time t; C_0 (mg/L) and C_t (mg/L) of chromium ion are the concentrations at time 0 and t, respectively; V is the solution volume (L); m is the mass of the mesoporous molecular sieves (g).

3. Results and discussion

3.1. Characterization of MCM-41 materials

Fig. 1 shows XRD patterns of synthesized MCM-41 sample. It is easy to observe that MCM-41 sample shows three resolved peaks including (100), (110) and (200). The (100) peak is characteristic peak of MCM-41 in XRD spectrum at $2\theta = 2.138°$ [24,25]. The $d_{(100)}$-spacing of 4.132 nm and unit cell parameter a_0

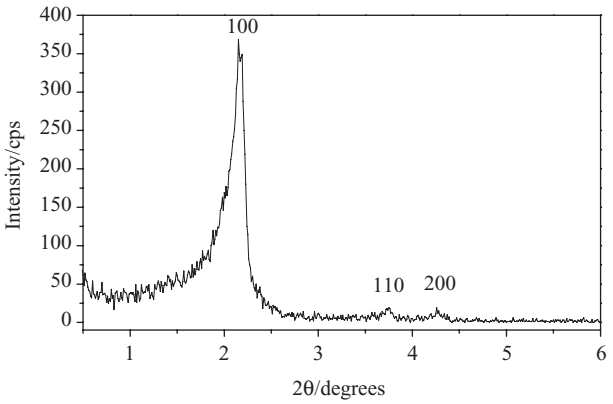

Fig. 1. XRD patterns of MCM-41.

of 4.771 nm were calculated from XRD spectrum in Table 1. Additionally, the (110) and (200) peaks are also strong diffraction peak. MCM-41 dose not have large crystals because of no diffraction peak in the region of higher angles (7–30°), which indicates synthesized MCM-41 is a good long-range order and crystallinity.

The characterization of MCM-41 also used nitrogen adsorption–desorption isotherms (a) and pore size distribution curves (b), as shown in Fig. 2. Fig. 2a shows nitrogen adsorption–desorption isotherms of MCM-41 are typical type-VI isotherms with a sharp infection at relative pressure P/P_0 approximately 0.25 which indicates capillary condensation of nitrogen within the uniform mesopore structure. Fig. 2b shows narrow pore size distribution (centered at 2.8 nm) of MCM-41, which can also demonstrate its uniformity of the size distribution. The synthesized MCM-41 with BET surface area (1040 m^2/g) and BJH pore diameter (2.8 nm) is typical values of surfactant-assembled mesostructures.

3.2. Effect of initial solution pH on Cr (VI) adsorption

Earlier studies have shown that solution pH is an important parameter that influences the adsorption of metal ions [20,26]. The adsorption efficiency is affected by the pH, as shown in Fig. 3. Cr (VI) adsorption on MCM-41 is strongly pH-dependent. At low pH (<4), adsorption efficiency increases with solution pH increasing and reaches the maximum (97.56%) at pH 4. Then it starts to decrease at pH > 5.

Cr (VI) can exist in several stable forms at different pH in the solution. The predominant molecules or anions are H_2CrO_4 at low pH (<1), $HCrO_4^-$ at pH 2–3, $HCr_2O_7^-$ and $Cr_2O_7^{2-}$ at pH 4–5 and CrO_4^{2-} at pH > 6 [27,28]. What's more, MCM-41 is very easy to adsorb the molecules and ions that are highly active and polar. So, we can see H_2CrO_4 and $HCrO_4^-$ with low activity and polarity are predominantly present at pH < 3. On the other hand, MCM-41 may not be stable at high acid solution. The adsorption efficiency is low and increases with pH increasing. When the pH ranges from 4 to 5, $HCr_2O_7^-$ and $Cr_2O_7^{2-}$ with higher activity and polarity are predominantly present in the solution. Additionally, each of them includes two chromium ions. So MCM-41 of a certain specific surface area must have high adsorption efficiency at pH 4–5. The activity of CrO_4^{2-} anions is low at pH > 6, so its adsorption efficiency begins to decrease, finally reaches equilibrium. Therefore, in the following experiments, we used an initial pH of 4.

3.3. Effect of adsorbent concentration on Cr (VI) adsorption

The effect of adsorbent concentration between 2 and 40 mg/L on Cr (VI) adsorption is shown in Fig. 4. Initially the adsorption efficiency increases greatly with an increase in adsorbent concentration, for example, the adsorption efficiency of 45.33% at 2 mg/L adsorbent concentration increases to 95.16% at 10 mg/L adsorbent concentration. But the adsorption efficiency only increases slowly when the adsorbent concentration is added more than 10 mg/L. This implies that the adsorption efficiency of per unit mass of adsorbent decreases. Similar results have previously been reported [29,30]. Lower adsorbent concentration will not remove Cr (VI) ions from solution completely, but higher adsorbent concentration will make the adsorbent wasteful. So an optimal adsorbent concentration of 10 mg/L by batch experiments is recommended.

3.4. Effect of initial chromium (VI) concentration on Cr (VI) adsorption

The initial chromium (VI) concentration is an important driving force to overcome the mass transfer resistance of metal ions between the aqueous and solid phase [31]. The effect of initial chromium (VI) concentration between 2.5 and 50 mg/L on the Cr (VI) adsorption is shown in Fig. 5. The adsorption efficiency decreases with the increase in the Cr (VI) concentration. For example, the adsorption efficiency of 99.86% at 2.5 mg/L Cr (VI) concentration decreases to 94.21% at 10 mg/L Cr (VI) concentration. But the adsorption efficiency starts to decrease greatly when Cr (VI) concentration is over 10 mg/L [32,33]. This may be due to an increase in the number of chromium (VI) ions competing for available binding sites on the surface of the adsorbent. The chromium (VI) ions once adsorbed onto MCM-41 will hinder latter ions adsorption and maybe exist repulsion between themselves. On the other hand, saturated adsorption capacity q of 904 mg/g calculated by Langmuir-linear fitting can

Table 1
Textural properties of the MCM-41

Sample	$d_{(100)}$/nm	Unit cell parameter a_0/nm	BJH Pore size/nm	BET Surface area/(m^2/g)
MCM-41	4.132	4.771	2.8	1040

where a_0 (nm) is the unit cell parameter ($a_0=2d_{(100)}/3^{1/2}$).

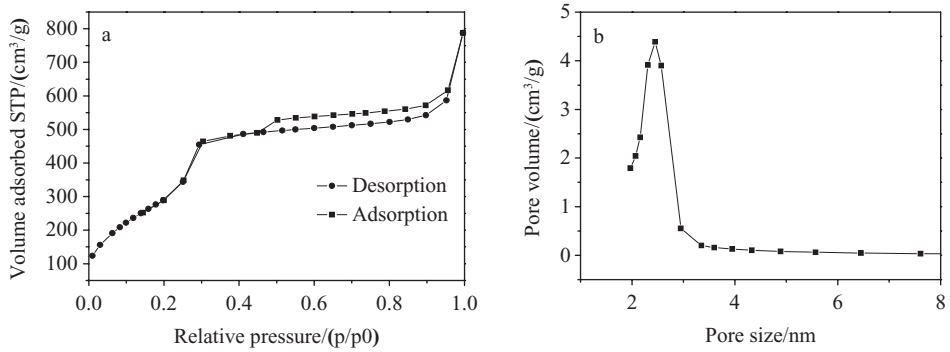

Fig. 2. Nitrogen adsorption-desorption isotherms (a) and pore size distribution curves (b) of MCM-41.

prove the truth that Cr (VI) concentration should be lower than 10 mg/L at 10 mg/L adsorbent concentration. So we think adsorption capacity of MCM-41 reaches the saturated state at 10 mg/L Cr (VI) concentration, which can make full use of the adsorption of mesoporous MCM-41. Cr (VI) concentration of 10 mg/L was used further on.

3.5. Effect of adsorption time on Cr (VI) adsorption

The adsorption time is an important parameter because it reflects the adsorption kinetics of the adsorbent for a given initial concentration of the adsorbate. The effect of adsorption time between 0.25 and 12 h on Cr (VI) adsorption is shown in Fig. 6. Initially, the adsorption efficiency increases rapidly, and then increases relatively slowly with adsorption time, finally reaches adsorption equilibrium (adsorption efficiency > 99%) after 2 h. Because there are both adsorption and desorption in the system. At the beginning, the adsorption is the predominant process. But desorption is enhanced and adsorption is weakened with the time, finally adsorption and desorption reach dynamic equilibrium. The adsorption efficiency

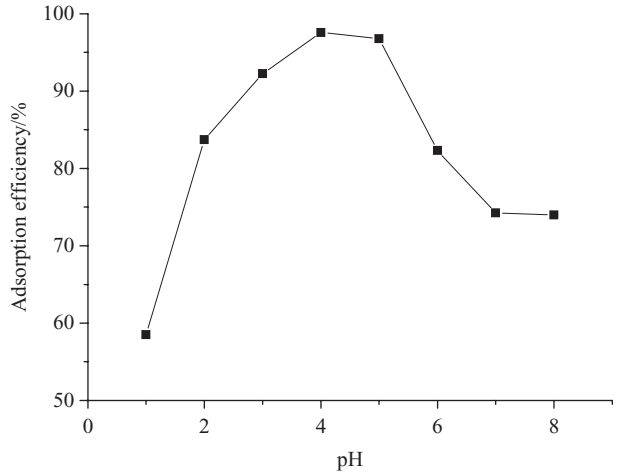

Fig. 3. Effect of initial pH on the adsorption efficiency of Cr (VI) onto MCM-41 using adsorbent concentration of 10 mg/L and Cr (VI) concentration of 10 mg/L at 25°C for 3 h.

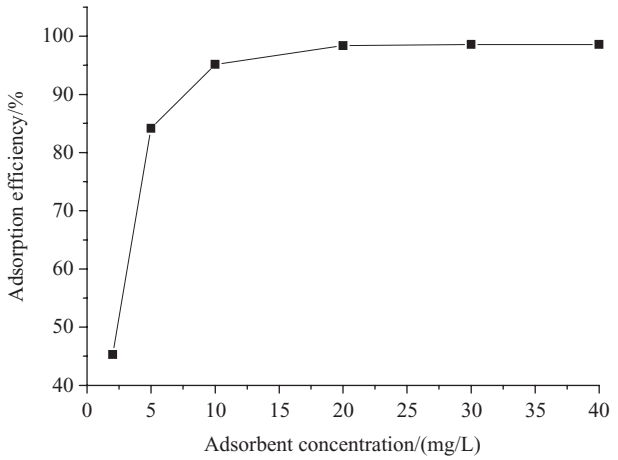

Fig. 4. Effect of adsorbent concentration on the adsorption efficiency of Cr (VI) onto MCM-41 at pH 4, Cr (VI) concentration of 10 mg/L and 25°C for 3 h.

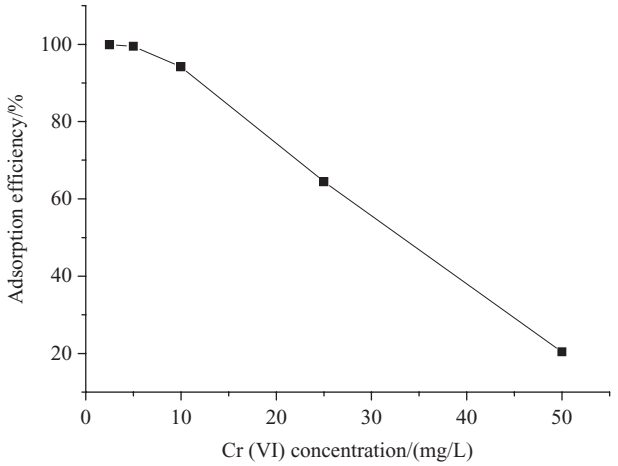

Fig. 5. Effect of initial Cr (VI) concentration on the adsorption efficiency of Cr (VI) onto MCM-41 at pH 4, adsorbent concentration of 10 mg/L and 25°C for 3 h.

was found to be higher than that of other adsorbents [34–37]. Therefore, an adsorption time of 2 h was found to be the optimum adsorption time without changing the other conditions.

3.6. Effect of temperature on Cr (VI) adsorption

The adsorption temperature is one of the most important parameters. The thermodynamic parameters can be calculated and are dependent on the temperature. Fig. 7 clearly indicates that Cr (VI) adsorption was optimum with an adsorption efficiency of 98.99% at 35°C. The adsorption of Cr (VI) onto the molecular sieve is endothermic and, therefore, the adsorption efficiency increases with increasing temperature. The activity of Cr (VI) ions increases and the chemical bond between

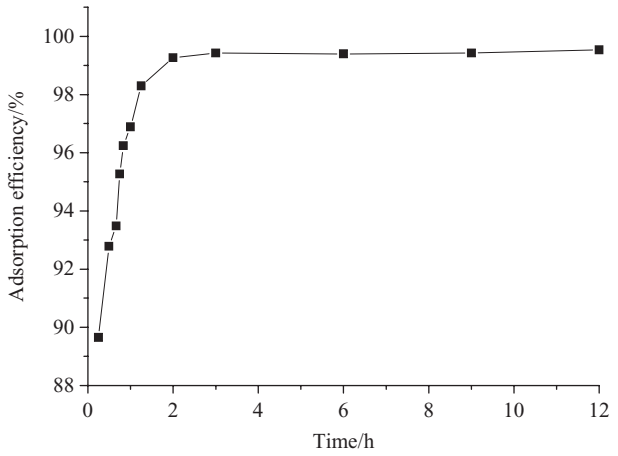

Fig. 6. Effect of adsorption time on the adsorption efficiency of Cr (VI) onto MCM-41 at pH 4, an adsorbent concentration of 10 mg/L, Cr (VI) concentration of 10 mg/L and 25°C.

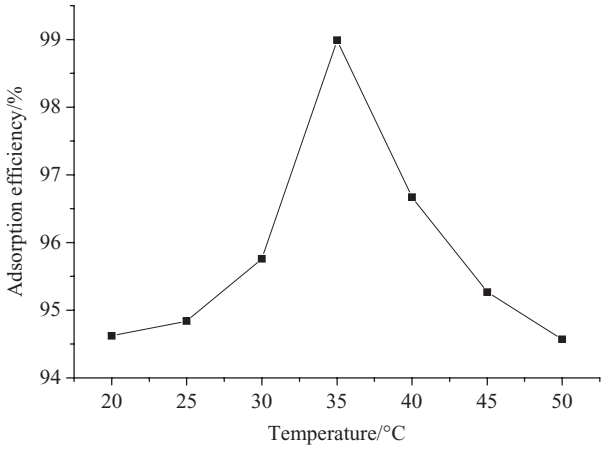

Fig. 7. Effect of temperature on the adsorption efficiency of Cr (VI) onto MCM-41 at pH 4, adsorbent concentration of 10 mg/L, Cr (VI) ion concentration of 10 mg/L and 2 h.

Cr (VI) and the molecular sieve begins to break with further temperature increase. So the adsorption efficiency decreases at temperature > 35°C and desorption becomes the main process [38,39]. MCM-41 adsorbs heavy metal ions at low temperature and desorbs them at high temperature. This implies that MCM-41 is easy to recycle at high temperature distillation.

3.7. Adsorption isotherm

For the isothermal adsorption process, the adsorption isotherm was investigated and predicted at 25°C. Of all the isothermal adsorption models, the Langmuir [40] and Freundlich [41] models are two of the most important.

The Langmuir and Freundlich adsorption isotherms can be expressed in linear form as follows:

$$\frac{C_e}{q_e} = \frac{C_e}{q} + \left(\frac{1}{bq}\right) \tag{3}$$

$$\ln q_e = \ln K_f + \left(\frac{1}{n}\right) \times \ln C_e \tag{4}$$

where q is the saturated adsorption capacity per unit mass of adsorbent (mg/g) and q_e is the equilibrium adsorption capacity per unit mass of adsorbent (mg/g); b (1/mg) and K_f ((mg/g)/(mg/L)$^{1/n}$) are equilibrium constants in Langmuir and Freundlich isotherms, respectively.

The adsorption isotherms were fitted by linear Langmuir and Freundlich fitting. The adsorption isotherms of the chromium ion are shown in Figs. 8 and 9.

From Figs. 8 and 9, the linear equations for the Langmuir and Freundlich fits are as follows: $C_e/q_e = 0.01442 + 1.10617C_e$, $r^2 = 0.9978$; $\ln q_e = -0.07781 + 0.02731 \ln C_e$,

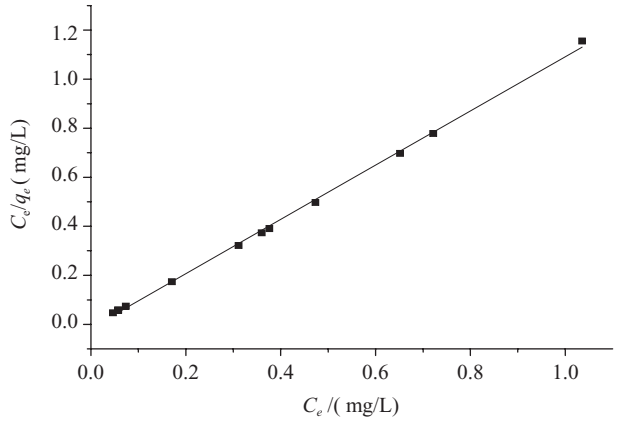

Fig. 8. Langmuir linear fit.

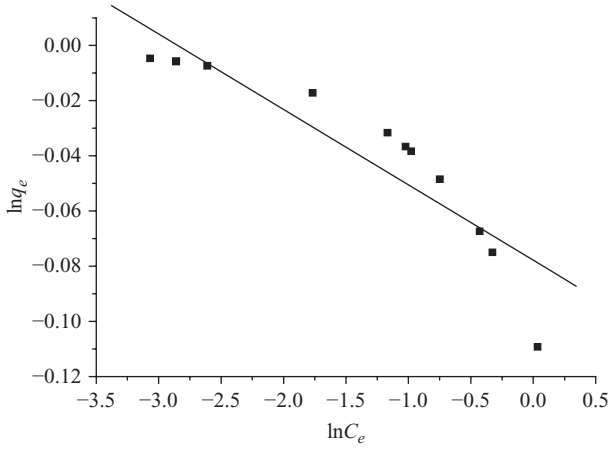

Fig. 9. Freundlich linear fit.

$r^2 = 0.7044$, where r^2 is the correlation coefficient. Therefore, the curves follow the Langmuir model better because the diameter size of MCM-41 is uniform and monolayer adsorption may occur. The b of 76.71 mg^{-1} and q of 904 mg/g were calculated by Langmuir-linear fitting. It is observed that adsorption capacity of MCM-41 is higher than other adsorbents from Table 2.

3.8. Adsorption thermodynamics

The Gibbs free energy change can be calculated as follows:

$$\Delta G^0 = -RT\ln K^0 = \Delta H^0 - T\Delta S^0 \quad (5)$$

$$\Delta H^0 = -R\left(\frac{T_2T_1}{T_2 - T_1}\right)\ln\left(\frac{K_2}{K_1}\right) \quad (6)$$

where K_0 is a equilibrium constant at standard state K_0 is equal to b at 25°C. K_1 and K_2 are the equilibrium constants at temperature T_1 (K) and T_2 (K), respectively.

We calculated Gibbs Free Energy Change at 298 and 308 K from the data shown in Figs. 6 and 7 and according to Eq. (5).
$\Delta G^0_{298K} = -1.0758\times10^4$ J mol^{-1}; $\Delta G^0_{308K} = -1.2168\times10^4$ J mol^{-1} and, therefore, ΔS^0 and ΔH^0 can be calculated from Eqs. (5) and (6). $\Delta S^0 = 141.08$ J mol^{-1} K^{-1}; $\Delta H^0 = 3.1305\times10^4$ J mol^{-1}.

The thermodynamic parameters were analyzed as follows: The negative value of ΔG^0 implies that the adsorption reaction is a spontaneous process. Furthermore, the decrease in ΔG^0 with an increase in temperature indicates that the adsorption is more spontaneous at higher temperature. A positive ΔH^0 means that the adsorption process is endothermic. The value of ΔH^0 (3.1305×10^4 J mol^{-1}) is close to 40 kJ mol^{-1} (this value is thought to be the upper limit of ΔH^0 for physical adsorption in general adsorption), which indicates the chemical adsorption of Cr (VI) onto MCM-41 may occur, but it should be studied in the future. A higher adsorption efficiency results from a higher temperature, but the adsorption efficiency does not increase at higher temperatures because desorption is favored at high temperature over adsorption. The positive ΔS^0 suggests that the system is more random at the solid/solution interface during the adsorption of Cr (VI) onto MCM-41. For the Cr (VI) adsorption process, the adsorbed solvent molecules that are displaced by the adsorbate species gain more translational entropy than that lost by the adsorbate ions, which leads to the prevalence of a more random system [38].

3.9. Adsorption kinetics

To examine the kinetics of the adsorption processes, pseudo first order and pseudo second order models were used to test the experimental data. The pseudo first order [42] and pseudo second order [43] equations can be expressed as follows:

$$\lg(q_e - q_t) = \lg q_e - \frac{k_1}{2.303}t \quad (7)$$

$$\frac{t}{q_t} = \frac{1}{k_2q_e^2} + \frac{t}{q_e} \quad (8)$$

where k_1 (h^{-1}) and k_2 (g mg^{-1} h^{-1}) are the rate constants of the pseudo first and pseudo second order adsorptions, respectively.

The pseudo first order and pseudo second order curves are shown in Figs. 10 and 11 using Eqs. (7) and (8). Experimental data is calculated from Fig. 6.

From Figs. 10 and 11, the pseudo first order and pseudo second order linear fitting results were determined to be: $\lg(q_e - q_t) = -1.81966 + 0.55396t$, $r^2 = 0.3400$

Table 2
Comparison of adsorption capacity of various adsorbents

Adsorbent	Model	q/(mg/g)	Reference
NH_2-MCM-41	Langmuir model	196.5	[18]
MCM-41	Langmuir model	185.2	[19]
Walnut hull	Langmuir model	98.13	[20]
Activated carbon	Freundlich model	7.5	[21]
Modified activated carbon	Freundlich model	14.5	[18]
Natural zeolite	Langmuir model	6.5	[36]
MCM-41	Langmuir model	904	This study

and $t/q_t = 0.04633+1.10426t$, $r^2 = 0.9996$, respectively. This curve better follows the pseudo second order model because of its high correlation coefficient (r^2=0.9996). The q_e and k_2 values calculated from these plots are 905.58 mg g^{-1} and 2.63×10^{-5} g mg^{-1} h^{-1} from Fig. 11 and Eq. (8), respectively. The q_e is close to the q_e (904 mg/g) calculated from Langmuir isotherm, which indicates Langmuir model can describe the adsorption isotherm better.

Adsorption kinetics is generally controlled by different mechanisms and usually consists of three stages [38,44]. In general, the last stage is considered to be fast enough. Firstly, heavy metal ions transfer from the solution through film diffusion to the surface of the adsorbent. Secondly, ion diffusion occurs from the material surface to the material bulk. Thirdly, ion chelation occurs on the reactive surface of the material bulk. Therefore, film diffusion [45], intra-particle diffusion [46] and actual adsorption step are in the process. The slowest phase is the control process. Neither the pseudo first order nor the pseudo second order model can describe the adsorption. The kinetic results thus need to be analyzed using three stages and they are:

$$\text{Intra}-\text{particle diffusion}: q_t = k_i t^{1/2} + c \quad (9)$$

where k_i (g mg^{-1} $h^{-1/2}$) is the intra-particle diffusion rate constant and c (mg g^{-1}) is a constant. k_i, c and the correlation coefficient were calculated from the plot of q_t versus $t^{1/2}$. We found that the correlation coefficient (r^2=0.87483) of the intra-particle diffusion model is very low as shown in Fig. 12. This indicates that the adsorption of Cr (VI) onto MCM-41 does not absolutely follow the intra-particle diffusion kinetics. Fig. 12 clearly shows that intra-particle diffusion kinetics includes three regions. Each region is a straight line, which seems to be three steps of the adsorption processes. The first step expresses Cr (VI) transfers from the solution through film diffusion to the outer surface of MCM-41 and this step is slow, which indicates a boundary layer effect. Secondly, Cr (VI) diffuses to MCM-41 bulk from the material surface, namely intra-particle and pore diffusion. This step is so fast. The third step is close to equilibrium state, so the slope of q_t versus $t^{1/2}$ is smooth. Cr (VI) concentration in the solution is extremely low leading to the film and intra-particle diffusion slowing down.

To explore the adsorption mechanism in detail and determine the actual rate-controlling step in the

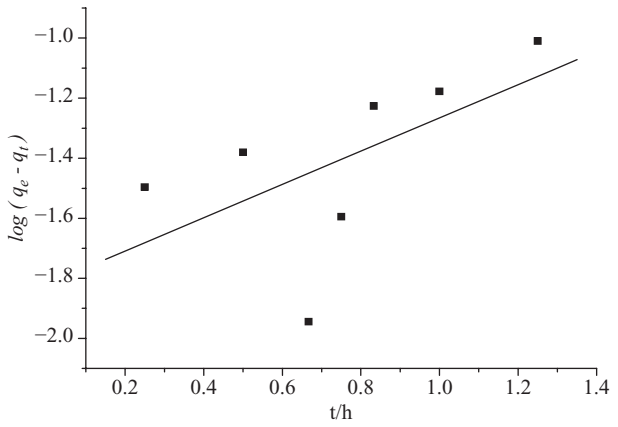

Fig. 10. Pseudo first order kinetic plot for the adsorption of Cr (VI) onto MCM-41.

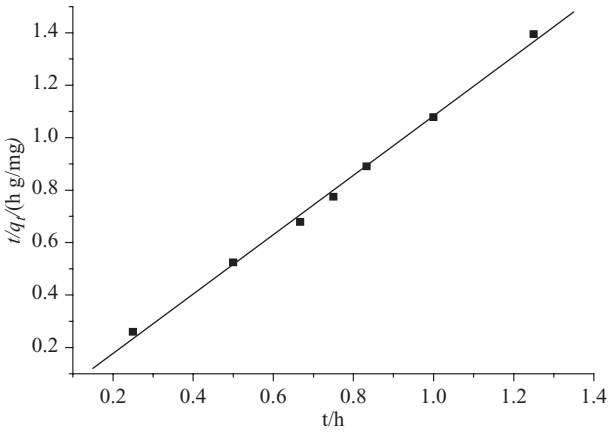

Fig. 11. Pseudo second order kinetic plot for the adsorption of Cr (VI) onto MCM-41.

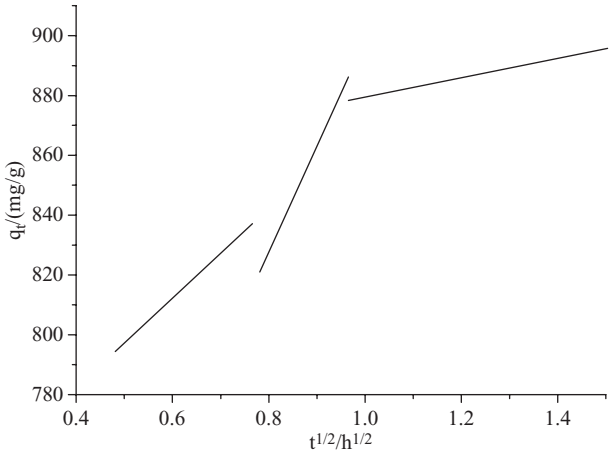

Fig. 12. Intra-particle diffusion kinetic plot for the adsorption of Cr (VI) onto MCM-41.

adsorption process, we used Eq. (10) from film diffusion dynamics.

$$F = 1 - \frac{6}{\pi^2}\sum_{1}^{\infty}\left(\frac{1}{n^2}\right)e^{(-n^2 B_t)} \tag{10}$$

where F is the fraction of solute adsorbed at different time t; n is the Freundlich constant of the adsorbate; B_t is a mathematical function of F, which is the degree of ion exchange and can be expressed as in Eq. (11):

$$F = \frac{q_t}{q_e} \tag{11}$$

Rearranging the above equation gives:

$$B_t = -0.4799 - \ln(1 - F) \tag{12}$$

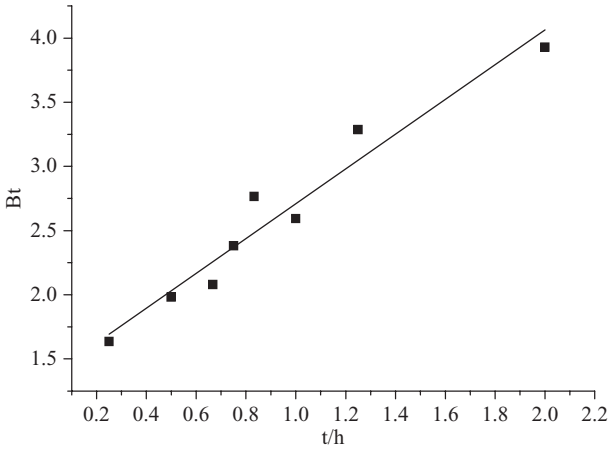

Fig. 13. B_t vs. t plot for the adsorption of Cr (VI) onto MCM-41.

Therefore, the value of B_t can be calculated for each F using Eq. (12). Fig. 13 shows the B_t value as a function of t. The linearity of this plot provides useful information to distinguish between film diffusion and intra-particle diffusion. If a plot of B_t vs. t is a straight line that passes through the origin, the adsorption will be governed by a particle-diffusion mechanism, otherwise it will be governed by film diffusion. Fig. 13 obvious shows that the plot of B_t vs. t is a straight line but it does not pass through the origin. The linear plot correlation coefficient (r^2=0.93822) is higher than the intra-particle correlation coefficient. This implies that Cr (VI) adsorption onto MCM-41 is mainly controlled by film diffusion along with a considerable contribution from the intra-particle diffusion mechanism [47–50].

4. Conclusions

Characterization results of synthesized MCM-41 show that it is a good adsorption material of good crystallinity, large surface area (1040 m^2/g) and uniform diameter (centered at 2.8 nm). Experiments of adsorbing Cr (VI) from aqueous solution indicate that adsorption efficiency of MCM-41 is high (maximum > 99%). The best Cr (VI) adsorption conditions were found at a pH of 4, a temperature of 35°C, an initial Cr (VI) concentration <10 mg/L, an adsorbent concentration of 10 mg/L and an adsorption time of 2 h from single-factor tests. In addition, removal of Cr (VI) is strongly pH-dependent, reaching a maximum (97.56%) at pH 4. Chromium ion adsorption isotherms were obtained at 25°C and then fitted to Langmuir and Freundlich models. The adsorption isotherms are more suited to the Langmuir model. From Langmuir linear fitting, saturated adsorption capacity q of 904 mg/g and adsorption equilibrium constant b of 76.71 mg^{-1} were calculated. The adsorption reaction of Cr (VI) onto MCM-41 is spontaneous and endothermic with $\Delta G^0 < 0$ and $\Delta H^0 > 0$. The adsorption capacity increases with increasing temperature. However, over 35°C, the Cr (VI) that adsorbs on the molecular sieve shows increased activity and then begins to desorb. The adsorption kinetics was studied using pseudo first and pseudo second order kinetic models. It is found that Cr (VI) adsorption onto MCM-41 better follows pseudo second order kinetics and its rate determining step is very complex, which is mainly controlled by the film diffusion mechanism along with a considerable contribution from the intra-particle diffusion mechanism.

References

[1] M.C. He, Z.J. Wang and H.X. Tang, The chemical, toxicological and ecological studies in assessing the heavy metal pollution in Le An River, China. Water Res., 32 (1998) 510–518.

[2] L. Rodriguez, E. Ruiz, J. Alonso-Azcárate and, J. Rincón, Heavy metal distribution and chemical speciation in tailings and soils around a Pb–Zn mine in Spain, J. Environ. Manage., 90 (2009) 1106–1116.
[3] K. Kolomaznik, M. Adamek, I. Andel and M. Uhlirova, Leather waste—Potential threat to human health and a new technology of its treatment, J. Hazard. Mater., 160 (2008) 514–520.
[4] H.D. Choi, W.S. Jung, J.M. Cho, B.G. Ryu, J.S. Yang and K. Baek, Adsorption of Cr (VI) onto cationic surfactant-modified activated carbon, J. Hazard. Mater., 166 (2009) 642–646.
[5] J.R. uan, S. Hernández, J.M. Andrés and C. Ruiz, Ion exchange uptake of ammonium in wastewater from a Sewage Treatment Plant by zeolitic materials from fly ash, J. Hazard. Mater., 161 (2009) 781-786.
[6] J.H. Hong, S.E. Duncan, S.F. Keefe and A.M. Dietrich, Ultrafiltration as a tool to study binding of copper to salivary proteins, Food Chem., 113 (2009) 180–184.
[7] S.J. Li, J.M. Zhuang., T.T. Zhi, H.L Chen and L. Zhang, Combination of complex extraction with reverse osmosis for the treatment of fumaric acid industrial wastewater, Desalination, 234 (2008) 362–369.
[8] S.S. Chen, C.W. Li, H.D. Hsu, P.C. Lee, Y.M. Chang and C.H. Yang, Concentration and purification of chromate from electroplating wastewater by two-stage electrodialysis processes, J. Hazard. Mater., 61 (2009) 1075–1080.
[9] R.S. Bai and T.E. Abraham, Studies on chromium (VI) adsorptione desorption using immobilized fungal biomass, Bioresour. Technol., 87 (2003) 17–26.
[10] M. Algarra, M.V. Jimenez, E.R. Castellon, A.J. Lopez and J.J. Jimenez, Heavy metals removal from electroplating wastewater by aminopropyl-Si MCM-41, Chemosphere, 59 (2005) 779–786.
[11] J. Aguado, J.M. Arsuaga, A.M. Arencibia and V.G. Lindo, Aqueous heavy metals removal by adsorption on amine-functionalized mesoporous silica, J. Hazard. Mater., 163 (2009) 213–221.
[12] L. Huang, Q.L. Huang, H.N. Xiao and M. Eić, Effect of cationic template on the adsorption of aromatic compounds in MCM-41, Microp. Mesop. Mater., 98 (2007) 330–338.
[13] S.C. Laha and R. Kumar, Promoter-induced synthesis of MCM-41 type mesoporous materials including Ti- and V-MCM-41 and their catalytic properties in oxidation reactions, Microp. Mesop. Mater., 53 (2002) 163–177.
[14] M. Anilkumar and W.F. HÖderich, Highly active and selective Nb modified MCM-41 catalysts for Beckmann rearrangement of cyclohexanone oxime to ϵ-caprolactam, J. Catal., 260 (2008) 17–29.
[15] J.M. Campos, M.R. Ribeiro, J.P. Lourenço and A. Fernandes, Ethylene polymerisation with zirconocene supported in Al-modified MCM-41: Catalytic behaviour and polymer properties, J. Mol. Catal. A: Chem., 277 (2007) 93–100.
[16] M. Selvaraj, P.K. Sinha, K. Lee, I. Ahn, A. Pandurangan and T.G. Lee, Synthesis and characterization of Mn–MCM-41 and Zr–Mn-MCM-41, Microp. Mesop. Mater., 78 (2005) 139–149.
[17] P. Mahitti and U. Fuangfa, Preparation and use of chemically modified MCM-41 and silica gel as selective adsorbents for Hg (II) ions, J. Hazard. Mater., 154 (2008) 578–587.
[18] K.F. Lam, K.L.Yeung and G. Mckay, Selective mesoporous adsorbents for $Cr_2O_7^{2-}$ and Cu^{2+} separation, Microp. Mesop. Mater., 100 (2007) 191–201.
[19] M. Ghiaci, R. Kia, A. Abbaspur and F. Seyedeyn-Azad, Adsorption of chromate by surfactant-modified zeolites and MCM-41 molecular sieve, Sep. Purif. Technol., 40 (2004) 285–295.
[20] X.S. Wang, Z.Z. Li and S.R. Tao, Removal of chromium (VI) from aqueous solution using walnut hull, J. Environ. Manage., 90 (2009) 721–729.
[21] F.D. Natale, A. Lancia, A. Molino and D. Musmarra, Removal of chromium ions form aqueous solutions by adsorption on activated carbon and char, J. Hazard. Mater., 145 (2007) 381–390.
[22] S.A. Bagshaw, E. Prouzet and T.J. Pinnavaia, Templating of mesoporous molecular sieves by nonionic polyethylene oxide surfactants, Science, 269 (1995) 1242–1244.
[23] J.Y. Ying, C.P. Mehnert and M.S. Wong, Synthesis and applications of supramolecular-templated mesoporous materials, Angew. Chem. Int. Ed., 38 (1999) 56–77.
[24] S. Wang, T. Dou, Y.P. Li, Y. Zhang, X.F. Li and Z.C. Yan, Synthesis, characterization and catalytic properties of stable mesoporous molecular MCM-41 prepared from zeolite mordenite, J. Solid State Chem., 177 (2004) 4800–4805.
[25] D.P. Quintanilla, A. Sánchez, I. Hierro, M. Fajardo and I. Sierra, Preparation, characterization, and Zn^{2+} adsorption behavior of chemically modified MCM-41 with5-mercapto-1-methyltetrazole, J. Colloid Interf. Sci., 313 (2007) 551–556.
[26] V.K. Gupta, A.K. Shrivastava and N. Jain, Biosorption of chromium (VI) from aqueous solutions by green algae Spirogyra species, Water Res., 35 (2001) 4079–4085.
[27] K.C. Luis, C.A. Ramelito, L.L. Johannes, O. Marcel and A.M. van der Wielen, Potential of Biosorption for the Recovery of Chromate in Industrial Wastewaters, Ind. Eng. Chem. Res., 40 (2001) 2302–2309.
[28] D.E. Kimbrough, Y. Cohen, A.M. Winer, L. Creelman and C. Mabuni, A critical assessment of chromium in the environment, Crit. Rev. Environ. Sci. Technol., 29 (1999) 1–46.
[29] V. Vimonses, S. Lei, B. Jin, W.K. Chris and S. Chris, Adsorption of congo red by three Australian kaolins, Appl. Clay Sci., 43 (2009) 465–472.
[30] S.S. Gupta and K.G. Bhattacharyya, Immobilization of Pb (II), Cd (II) and Ni (II) ions on kaolinite and montmorillonite surfaces from aqueous medium, J. Environ. Manage., 87 (2008) 46–58.
[31] G. Dönmez and Z. Aksu, Removal of chromium (VI) from saline wastewaters by Dunaliella species, Process. Biochem., 38 (2002) 751–762.
[32] S.S. Gupta and K.G. Bhattacharyya, Adsorption of Ni (II) on clays, J Colloid Interf. Sci., 295 (2006) 21–32.
[33] F.D. Ardejani, K. Badii, N.Y. Limaee, S.Z. Shafaei and A.R. Mirhabibi, Adsorption of Direct Red 80 dye from aqueous solution onto almond shells: Effect of pH, initial concentration and shell type, J. Hazard. Mater., 151 (2008) 730–737.
[34] G.E. Boyd, A.W. Adamson and L.S. Mayers, The exchange adsorption of ions from aqueous solution by organic zeolites II Kinetics, J. Am. Chem. Soc., 69 (1947) 2836–2848.
[35] M.J. Sánchez-Martín, M.C. Dorado, C.D. Hoyo and M.S. Rodríguez-Cruz, Influence of clay mineral structure and surfactant nature on the adsorption capacity of surfactants by clays, J. Hazard. Mater., 150 (2008) 115–123.
[36] T. Motsi, N.A. Rowson and M.J.H. Simmons, Adsorption of heavy metals from acid mine drainage by natural zeolite, Int. J. Miner. Process., 92 (2009) 42–48.
[37] S.B. Wang, H.T. Li and L.Y. Xu, Application of zeolite MCM-22 for basic dye removal from wastewater, J. Colloid Interf. Sci., 295 (2006) 71–78.
[38] W. Makowski and P. Kus'trowski, Probing pore structure of microporous and mesoporous molecular sieves by quasi-equilibrated temperaturenext term programmed previous term-desorption and adsorptionnext term of n-nonane, Microp. Mesop. Mater., 102 (2007) 283–289.
[39] H. Cui and S.Q. Turn, Adsorption/desorption of dimethylsulfide on activated carbon modified with iron chloride, Appl. Catal. B: Environ., 88 (2009) 25–31.
[40] I. Langmuir, The adsorption of gases on plane surfaces of glass, mica and platinum, J. Am. Chem. Soc., 40 (1918) 1361–1403.
[41] H.M. Freundlich, Ueber die adsorption in loesungen, Z. Phys. Chem., 57 (1906) 385–470.
[42] S. Lagergren, Zur theorie der sogenannten adsorption geloster stoffe, Kungliga Svenska Vetenskapsakademiens, Handlingar, 24 (1898) 1–39.
[43] Y.S. Ho and G. McKay, Kinetic models for the sorption of dye from aqueous solution by wood, Pro. Safe Environ. Pro., 76 (1998) 183–191.

[44] C. Namasivayam and K. Ranganathan, Waste Fe (III)/Cr (III) hydroxide as adsorbent for the removal of Cr (VI) fromaqueous solution and chromium plating industry wastewater, Environ. Pollut., 82 (1993) 255–261.
[45] W.J. Weber and J.C. Morris, Kinetics of adsorption on carbon from solution, J. San.Eng. Div. ASCE, 89 (1963) 31–59.
[46] D. Reichenberg, Properties of ion-exchange resins in relation to their structure III kinetics of exchange, J. Am. Chem. Soc., 75 (1953) 589–592.
[47] H. Chen and A.Q. Wang, Adsorption characteristics of Cu (II) from aqueous solution onto poly (acrylamide)/attapulgite composite, J. Hazard. Mater., 165 (2009) 223–231.
[48] D. Mohan, V.K. Gupta, S.K. Srivastava and S. Chander, Kinetics of mercury adsorption from wastewater using activated carbon derived from fertilizer waste, Colloids Surf. A Physicochem. Eng. Asp., 177 (2001) 169–181.
[49] C. Valderrama, X. Gamisans, X. de las Heras, A. Farŕan and J.L. Cortina, Sorption kinetics of polycyclic aromatic hydrocarbons removal using granular activated carbon: Intraparticle diffusion coefficients, J. Hazard. Mater., 157 (2008) 386–396.
[50] D. Mohan, K.P. Singh, S. Sinha and D. Gosh, Removal of pyridine from aqueous solution using low cost activated carbons derived from agricultural waste materials, Carbon, 42 (2004) 2409–2421.